Nuclide analysis in high burnup fuel samples irradiated in Vandellós 2

H.U. Zwicky [a,*], J. Low [b], M. Granfors [b], C. Alejano [c], J.M. Conde [c], C. Casado [d], J. Sabater [d], M. Lloret [d], M. Quecedo [d], J.A. Gago [e,1]

[a] Zwicky Consulting GmbH, Chilacherstr. 17, 5236 Remigen, Switzerland
[b] Studsvik Nuclear AB, 611 82 Nyköping, Sweden
[c] Consejo de Seguridad Nuclear, Justo Dorado 11, 28040 Madrid, Spain
[d] ENUSA, Santiago Rosiñol 12, 28040 Madrid, Spain
[e] ENRESA, Emilio Vargas 7, 28043 Madrid, Spain

ARTICLE INFO

ABSTRACT

In the framework of a high burnup fuel demonstration programme, rods with an enrichment of 4.5% ^{235}U were operated to a rod average burnup of about 70 MWd/kgU in the Spanish Vandellós 2 pressurised water reactor. The rods were sent to hot cells and used for different research projects. This paper describes the isotopic composition measurements performed on samples of those rods, and the analysis of the measurement results based on comparison against calculated values.

The fraction and composition of fission gases released to the rod free volume was determined for two of the rods. About 8% of Kr and Xe produced by fission were released. From the isotopic composition of the gases, it could be concluded that the gases were not preferentially released from the peripheral part of the fuel column.

Local burnup and isotopic content of gamma emitting nuclides were determined by quantitatively evaluating axial gamma scans of the full rods. Nine samples were cut at different axial levels from three of the rods and analysed in two campaigns. More than 50 isotopes of 16 different elements were assessed, most of them by Inductively Coupled Plasma Mass Spectrometry after separation with High Performance Liquid Chromatography. In general, these over 400 data points gave a consistent picture of the isotopic content of irradiated fuel as a function of burnup. Only in a few cases, the analysis provided unexpected results that seem to be wrong, in most cases due to unidentified reasons. Sample burnup analysis was performed by comparing experimental isotopic abundances of uranium and plutonium composition as well as neodymium isotopic concentrations with corresponding CASMO based data. The results were in agreement with values derived independently from gamma scanning and from core design data and plant operating records.

Measured isotope abundances were finally assessed using the industry standard SAS2H sequence of the SCALE code system. This exercise showed good agreement between measured and calculated values for most of the analysed isotopes, similar to those reported previously for lower burnup ranges. Thus, it could be concluded, that SAS2H results for high burnup samples are not subject to higher uncertainty and/or different biases than for lower burnup samples, and that the different isotopic experimental measurement methods provide accurate results with acceptable precision.

1. Introduction

Nuclide analyses in irradiated fuel are often performed within commercial post-irradiation projects. Consequently, there is a lack of published data, in particular on high burnup fuel irradiated under representative conditions.

Chemical analysis of dissolved pellet samples is one of the key methods to be applied in post-irradiation examination of irradiated fuel. Amongst others, it forms the basis for burnup determination, for physics codes benchmarking and for establishing nuclide inventories important for burnup credit assessment for intermediate storage of spent fuel and for back-end risk analysis. Isotope Dilution Analysis with chemical separation of elements of interest, followed by isotopic analysis with a Thermal Ionisation Mass Spectrometer (TIMS) is a well established method providing very accurate and precise results. Because this method is very time-consuming, it has become more and more common to introduce alternative techniques, e.g. High Performance Liquid Chromatography (HPLC) for elemental separations, combined with Inductively Coupled Plasma Mass Spectrometry (ICP-MS). In general, these

---

* Corresponding author. Tel.: +41 56 284 16 94; fax: +41 56 284 16 93.
E-mail address: hans-urs.zwicky@bluewin.ch (H.U. Zwicky).
[1] Present address: Endesa, Ribera del Loira, 60, 28042 Madrid, Spain.

alternative methods are somewhat less precise. This disadvantage is at least partly compensated by the possibility of analysing a larger number of nuclides and samples.

Normally, the axial profile of gamma emitting nuclides is measured as part of hot cell examinations of irradiated fuel rods. As pellet–pellet interfaces are well visible in detailed plots of such data, the profiles provide important information for cutting samples for destructive characterisation. Moreover, as a complement to chemical methods, quantitative evaluation of the measured data allows determining local burnup values and isotope concentrations.

Before cutting the rods into segments for further characterisation, some rods were punctured and the amount of gas in the free rod volume was determined. The composition of the gas was determined by gas mass spectrometry and the portion of released fission gases assessed.

The present project aimed at providing nuclide data suitable for benchmarking models, important for reactor operation as well as for intermediate storage and final disposal. It was performed in the framework of a high burnup fuel demonstration programme with rods fabricated by ENUSA and irradiated in the Spanish Vandellós 2 pressurised water reactor. Nuclide analyses in dissolved fuel samples were performed in Studsvik in two campaigns, the first one in 2003 on seven samples from two different fuel rods, the second one in 2006/2007, re-analysing on one hand solutions from the first campaign, on the other hand characterising two additional samples dissolved by alternative methods. Moreover, different analysing equipment was used in the second campaign.

2. Selected isotopes

The list of nuclides measured in this project is included in Table 1. The nuclides have been selected on the basis of their importance for criticality safety, radiation shielding and residual heat calculations, as described in [1]. However, some relevant nuclides have been excluded due to practical reasons. This has been the case for some metallic isotopes that have an important reactivity worth, but for which a reliable concentration measurement is difficult. Not all listed isotopes have been analysed in all samples.

3. Fuel samples

Fuel rods with an initial ^{235}U enrichment of 4.5 wt.% with three different cladding material types were fabricated by ENUSA and irradiated to a rod average burnup of about 70 MWd/kgU in the

Table 1
List of analysed nuclides.

Element	Atomic mass of analysed nuclides						
U	233[a]	234	235	236	238		
Np	237						
Pu	238	239	240	241	242		
Am	241	243					
Cm	244	246					
Mo	95	97	98	100			
Tc	99						
Ru	103	106					
Rh	103						
Cs	133	134	135	137			
La	139						
Ce	140	142	144				
Nd	142	143	144	145	146	148	150
Sm	147	148	149	150	151	152	154
Eu	151	153	154	155			
Gd	154	155	156	157	158	160	

[a] Reported as sample-specific detection limit.

Table 2
Sample information.

Rod	Sample	Position[a] (mm)	Local burnup[b] (MWd/kgU)	Remarks
WZR0058	E58-88	88–90	44.5	Analysed in 1st campaign
	E58-148	148–150	54.3	Analysed in 1st and 2nd campaign
	E58-257	252–262.5	64.9	Analysed in 2nd campaign
	E58-263	263–265	64.9	Analysed in 1st campaign
	E58-773	773–775	76.2	Analysed in 1st campaign
	E58-793	793–795	76.2	Analysed in 1st and 2nd campaign
	E58-796	796–798	76.2	Analysed in 1st campaign
WZtR160	WZtR160-800	792–802.5	72.5	Analysed in 2nd campaign
WZtR165	WZtR165-2a	1060–1062	78.2	Analysed in 1st campaign

[a] From bottom end of rod.
[b] Based on gamma scanning.

Spanish Vandellós 2 pressurised water reactor during cycles 7–11, between June 1994 and September 2000 in the framework of a high burnup fuel demonstration programme. During cycles 7–10, the rods were located in four different assemblies operated in equivalent symmetry positions. For their last cycle, the rods were removed from their original assemblies and inserted into different positions of the same bundle. Slight differences in burnup were caused by the different rod positions within the fuel assemblies, in particular during cycle 10, when the assemblies were located at the periphery of the core.

In total, nine samples were cut from three different rods and analysed in two campaigns in 2003 and in 2006/2007, respectively. Sample designations, positions and approximate burnup values are compiled in Table 2.

4. Applied methods

4.1. Fission gas release

Fission gas release was determined in rods WZtR165 and WZR0058. The rods were punctured in the plenum. The internal gas was expanded into a standard volume and the resulting pressure was determined. Samples of the gas were collected for analysis by mass spectrometry. The total internal free volume of the rod was determined by the backfill method, using argon at constant pressure. The fission gas release fraction was calculated from the experimentally determined amount of xenon and krypton extracted from the rod and the ORIGEN calculated total inventory of fission gases generated in the fuel over its entire irradiation.

After puncturing, the rods were cut into segments before they were further investigated.

4.2. Gamma scanning

A high purity germanium detector behind a 0.5 mm tungsten collimator was used for the measurements. Axial gamma scanning was performed applying the technique of closely spaced point measurements.

The efficiency file for the detector and collimator system was calibrated to give photon energy independent activity values for

a fuel rod with an outer diameter of 9.5 mm with no extra absorber. Activities were decay-corrected to the end of irradiation.

A well characterised reference rod was scanned together with the segments. By comparing the apparent ^{137}Cs activity measured for the reference rod with the decay-corrected ^{137}Cs activity known from the characterisation of the rod, a correction factor to be applied on all apparent activities was determined. The geometry of the reference rod was very similar to Vandellós 2 rods. Therefore, no extra correction of geometrical differences was necessary. Dead time correction of the system was checked by following the signal from a ^{60}Co source placed close to the detector. No extra correction was necessary.

The absolute activity was determined according to the following general formula:

$$a = \bar{a} \cdot c \cdot \frac{1}{f(E_\gamma)} \cdot g \cdot d$$

with a is the absolute activity (Bq/mm), $\bar{a}$ the apparent (measured) activity (Bq/mm), f the absorption factor, E_γ the Energy peak, g the geometry factor, d the dead time correction factor, c the ^{137}Cs reference rod correction: $c = \frac{a_{RR}(t_{ref})}{\bar{a}_{RR}(t_{ref})}$, a_{RR} the activity of reference rod, $\bar{a}_{RR}$ the apparent (measured) activity of reference rod and t_{ref} is the time at end of irradiation of the rod being scanned

Rod WZtR165 was scanned in May 2001, rod WZR0058 (up to about 3400 mm from lower end of fuel column) in April/May 2002. ^{95}Nb, ^{103}Ru (WZtR165 only), ^{106}Ru, ^{154}Eu, ^{134}Cs, ^{137}Cs, ^{144}Ce and ^{144}Pr were measured. The distance between individual measurements was 0.5 mm for rod WZR0058 and 0.25 mm for rod WZtR165. The lowermost segment of rod WZtR160, about 1500 mm long, was scanned in May 2006 with a step width of 0.25 mm. Due to the long decay time, only ^{137}Cs, ^{134}Cs and ^{154}Eu could be measured.

The gamma scan results from the positions of the samples for nuclide analysis were transformed into amount of nuclide ^nX in weight percent relative to ^{238}U. The amount of measured nuclides was determined from the average activity per length unit (Bq/mm) calculated from the gamma scan data. Values from pellet–pellet interfaces were excluded. The amount of ^{238}U per length unit of unirradiated fuel was determined, based on pre-irradiation data (density, stoichiometry, enrichment). The residual ^{238}U per length unit at the end of the irradiation was estimated based on CASMO calculations, neglecting the irradiation-induced change of the fuel stack length, which uses to be <1%.

4.3. Chemical analysis

4.3.1. Dissolution

In the first campaign, the fuel sample, consisting of a 2 mm long slice, was placed in a glass flask together with 20 ml of concentrated HNO_3 and kept at 65 °C for 6 h. Evaporation of liquid was avoided by means of an air-cooled reflux cooler. Nitrogen was bubbled through the liquid in order to stir it. The fuel matrix together with all fission products of interest went into solution. The cladding and the metallic fission product inclusions remained undisclosed.

The two 10 mm samples E58-257 and WZtR160-800, dissolved in the second campaign, were each cut in two pieces and dissolved in a 4748 Large Capacity Bomb from Parr Instrument Company.[2] This high pressure bomb has a capacity of 125 ml and can be used at 250 °C with a pressure of 1900 psig. It contains a removable PTFE cup in a stainless steel body with six cap screws in the screw cap to seal the flanged PTFE cup. An expandable wave spring maintains continuous pressure on the seal during the cooling cycle

when PTFE parts might otherwise relax and leak. A safety rupture disc above the PTFE cup protects the bomb from excessive overpressure. The oven for heating the bomb was constructed and built at Studsvik. It is made of brass and steel. The resistive heating is controlled by a thermostat.

The two pieces of sample E58-257 were each dissolved in 20 ml of a 2:1 mixture of concentrated HCl and HNO_3 during 6 h at 200 °C. The cladding was found to have disintegrated, with only a few larger pieces left. A grey residue was found on the bottom of the container. Therefore, the two pieces of sample WZtR160-800 were dissolved in two steps, first in 15 ml HNO_3 (suprapur) during 4 h at 180 °C. After removal of the cladding ring, alloy particles were dissolved by adding 30 ml concentrated HCl, followed by a second heat-up to 200 °C for 4 h. All solutions were combined in one single flask.

In the order of 0.1–0.4 g of the original fuel solution was diluted into 100 ml of HNO_3 (7.5 M) in the hot cell. Twenty millilitre of this solution were transferred to the laboratory. An appropriate aliquot was diluted with 100 ml HNO_3 (0.16 M) to a target uranium concentration of about 4 µg/g. The uranium concentration was determined by Scintrex analysis. The Scintrex[3] UA-3 is a uranium analyser, measuring the characteristic fluorescence of the uranyl ion in solution after irradiation with a very short pulse of ultraviolet light from a nitrogen laser. Thirty grams of this solution was then mixed with all necessary spike solutions.

4.3.2. The HPLC–ICP-MS instruments

During the first campaign, a DIONEX DX300 High Performance Liquid Chromatography (HPLC) system with an IonPac CG10 (4 × 50 mm) guard and an IonPac CS10 (4 × 250 mm) analytical column was used for the separations. The eluents were directly injected into a VG ELEMENTAL Plasmaquad PQ2+ Inductively Coupled Plasma Mass Spectrometer (ICP-MS), installed in a glove box. Details can be found in [2].

Different equipment was used in the second campaign. A DIONEX SP Gradient HPLC system and Autosampler Dionex AS with an IonPac CG10 (4 × 50 mm) guard and an IonPac CS10 (4 × 250 mm) analytical column was used for the separations. Chromeleon Xpress, CHX-1 software was used to control the autosampler, injector and HPLC pump. The eluents were directly injected into a Perkin Elmer Elan 6100 DRC II ICP-MS instrument, installed in a glove box. The ICP-MS instrument is controlled by Perkin Elmer Chromera software. The Chromera software was also used for the collection and evaluation of the chromatograms. Peak areas were used for the evaluation.

4.3.3. ICP-MS analysis based on one-point calibration

In this mode of analysis, count rates from an aliquot of the sample solution that is diluted as appropriate were compared to count rates from multi-element standard solutions. The first step in the evaluation of the data consisted of normalising all count rates to each other by means of added internal standards (^{115}In, ^{209}Bi). Blank corrections were performed by means of measurements of a pure diluted HNO_3 solution (0.16 M) preceding the analysis of each sample and standard solution. Average values were then compared to the corresponding average values measured in the standard solutions. Based on the known concentration of the nuclide in the standard, the concentration of the nuclide in the sample was calculated.

This mode of analysis is restricted to isotopes without any isobaric overlap. ^{99}Tc, ^{133}Cs, ^{135}Cs, ^{139}La, ^{237}Np as well as ^{244}Cm and ^{246}Cm, together with some nuclides analysed by Isotope Dilution

---

Analysis (IDA) as well, were determined by this method.

4.3.4. Isotope dilution analysis

IDA is based on the addition of a known amount of an enriched isotope ("spike") to a sample. Isotopic ratios between the added isotope and the isotope to be analysed are determined by mass spectrometry in the mixture of spike and sample, in the sample and, if not already known, in the spike. The amount of the isotope to be determined in the sample can be calculated from the isotopic ratios and the number of added spike atoms.

Identities of spike isotopes and of isotopes to be analysed, as well as their abundance in the corresponding spike solutions, are shown in Table 3.

Uranium isotopes were determined by IDA based on ICP-MS without separation. The measurements were performed in the peak jump mode.

Plutonium and americium isotopes were determined by IDA based on HPLC-ICP-MS, with an elution programme separating the two elements from each other and from interfering elements, e.g. uranium. In a separate run, the lanthanides cerium, neodymium, samarium, europium and gadolinium were determined. Caesium was separated from barium as cation.

Count rates measured in the analysis of uranium were blank corrected. The count rates from the unspiked and spiked samples of mass 238 were corrected for the contribution of ^{238}Pu, based on the count rate for mass 239 and the ratio of ^{238}Pu and ^{239}Pu determined in the plutonium analysis. The abundance of uranium isotopes in the unspiked sample was determined by normalising the corresponding count rates of five individual measurements to 100%, followed by calculating an average value for each individual isotope. The abundance of nuclides determined by HPLC-ICP-MS was calculated from the results of three individual runs. Isotopic ratios in the spiked solutions were calculated directly from the corresponding count rates or peak areas.

The number of atoms in the sample solution was transformed into micrograms. Finally, the amount of nuclide ^{n}X in weight percent relative to ^{238}U was calculated by dividing the corresponding amount by the amount of ^{238}U.

Besides stable isotopes with short-lived mother nuclides, chemical analyses included radioactive nuclides and nuclides with long-lived mother nuclides as well. In these cases, the analysed value is reported together with a value that was decay-corrected back to the end of the irradiation. All applied half-lives are compiled in Table 4. All values applied for correcting chemical analysis data were taken from [3]. The reference for half-lives applied in gamma scanning is not known. In the case of ^{154}Eu, the different half-lives introduce a potential systematic deviation of <2%.

4.4. Burnup analyses

One of the traditional methods for determining the burnup of irradiated LWR fuel is the ^{148}Nd method according to ASTM E 321 [4]. Probably one of the largest sources for systematic errors in this method is the assumed fission yield, requiring knowledge of the fraction of fissions occurring in ^{238}U (fast neutron fission) and ^{235}U, ^{239}Pu and ^{241}Pu (thermal). Another traditional method for burnup determination is based on the uranium and plutonium isotopic composition (ASTM E 244 [5]); this method is rarely used for LWR fuel due to its rather simplified and rough assumptions regarding the neutron spectrum and fission fractions (the standard has been withdrawn in 2001). However, modern physics codes like CASMO and HELIOS are instead able to calculate the amount of fission products and actinides formed or consumed during reactor operation in a much more sophisticated way, taking changes of irradiating conditions into account in a more detailed way than in the ASTM E 321 and ASTM E 244 methods. The uncertainty of these methods can therefore be eliminated to a certain extent, if the experimentally determined amount of suitable fission products or actinides is compared to the result of, e.g. CASMO calculations. Cross sections applied for CASMO calculations of isotope number densities are in general well known, at least in the case of fission products that are candidates for being used for burnup determination. The accuracy of CASMO results depends primarily on the quality of modelling operating history. In the case of the Vandellós 2 high burnup programme, operation was well documented, thus allowing a quite detailed modelling. Therefore, the error of CASMO calculations is assumed to be smaller than experimental errors. The method is described in [6].

Based on detailed information on operating conditions, number densities of all actinide and fission product isotopes of interest were calculated as a function of burnup by CASMO. The number densities were transformed into $^{n}X/^{238}$U values. Experimentally determined values for ^{146}Nd, ^{148}Nd and ^{150}Nd were compared to the calculated values, thus allowing a determination of the local pellet burnup. In addition, local pellet burnup was determined by comparing ^{235}U and ^{239}Pu isotopic abundances analysed by ICP-MS to isotopic abundances calculated from CASMO number densities.

Burnup was determined as well on the bases of ^{137}Cs activities measured by gamma scanning in the analysed rod and in the reference rod. The decay of ^{137}Cs during irradiation was calculated based on real power histories.

4.5. SAS2H calculations

The well known (industry standard) SAS2H sequence of the SCALE code system [7] was used to assess the measured nuclide inventories for the sample rods WZR0058 and WZtR165, as they

Table 3
Abundances of spike isotopes and isotopes to be analysed in spike solutions.

Spike isotope	Abundance (%)	Analysed isotope	Abundance (%)
^{233}U	98.043	^{238}U	0.804
^{242}Pu	99.903	^{239}Pu	0.0826
^{243}Am	99.966[a]	^{241}Am	0.031[a]
	99.967[b]		0.030[b]
^{96}Mo	95.60	^{97}Mo	1.03
^{133}Cs	100.00	^{137}Cs	–
^{140}Ce	99.30	^{142}Ce	0.70
^{148}Nd	91.60	^{146}Nd	2.50
^{154}Sm	99.02	^{152}Sm	0.473
^{151}Eu	99.24	^{153}Eu	0.76
^{155}Gd	91.6	^{156}Gd	6.34

[a] Reference date: April 12, 1984.
[b] Calculated for February 2007.

Table 4
Half-lives applied for decay corrections.

Nuclide	^{241}Pu	^{244}Cm	^{106}Ru	^{134}Cs	^{137}Cs	^{144}Ce	^{147}Pm	^{154}Eu	^{155}Eu
Half-life	14.35 a	18.10 a	*1.02 a*	2.06 a	30.17 a	284.8 d	2.62 a	8.8 a	4.761 a
				2.062 a	*30.1 a*	*284.2 d*		*8.5 a*	

Italic: *Applied in gamma scanning*

were provided in Refs. [8,9]. The aim of this analysis was twofold:

(1) serve as an independent validation check for the results obtained with a new measurement technique and
(2) identify potential limitations and/or biases of this widely used tool to accurately predict isotopic inventories for high burnup fuel. The results obtained will be presented and discussed in Section 5.3.

The SAS2H control module performs fuel irradiation and decay analysis through the execution of different functional modules and using input data from different burnup cross sections libraries included in the SCALE system.

The flux sequence used by SAS2H invokes first the execution of the functional modules BONAMI-S, NITAWL-II and XSDRNPM-S to produce cell-weighted cross sections for the fuel depletion calculations inside an infinite medium. These cross sections are later on used inside a large unit cell (e.g. an assembly) to take account of the heterogeneities introduced by the presence of water holes and the assembly guide tubes. The corrected cross sections updated by the COUPLE functional module are finally used in the ORIGEN-S module to calculate nuclide inventory variations of the irradiated fuel and the subsequent decay after discharging the fuel assembly from the reactor.

Other input data required to perform the sample isotopic analysis with SAS2H includes the specific burnup history of the sample, the fuel temperature, the moderator temperature and density, the boron curves and the power operation factors for each sample rod. Best estimate values for all these inputs were obtained from the plant records and/or from the core design values for the operating cycles were the two rods were irradiated.

The burnup for each sample was obtained from the calculated fuel rod burnup profile, corrected, when necessary, with plant flux map measured data. The estimated burnup for each sample is shown in the last column of Table 10. The sample burnups obtained by this method are consistent with the independent burnup estimations based on ^{235}U and ^{239}Pu inventories described in Section 4.4 and, therefore, it is concluded that those values are accurate enough to be used for the isotopic analysis presented in Section 5.3.

5. Results and discussion

5.1. Released fission gases

The result of the fission gas analyses is compiled in Table 5. Fission gas release was calculated assuming two different amounts of energy released per fission. With about 8% of the amount produced during operation, the fractional release of fission gases is in good agreement to published data. In rods containing fuel with an initial enrichment of 3.5–4.2%, operated in 15 × 15 fuel assembly geometry in a commercial PWR at somewhat higher average linear heat rates than the Vandellós high burnup rods, about 10–15% released fission gases were found at 70–80 MWd/kgU burnup [10].

Some isotopic ratios calculated from analysed data are compiled in Table 6 together with ratios based on CASMO data and on cumulative yields in thermal neutron fission of ^{235}U and ^{239}Pu [11]. As these ratios differ significantly in ^{235}U and ^{239}Pu fission, the ratio of U and Pu fissions can be estimated. About one third of the released fission gases was produced in Pu fissions. The composition of the released gases is the same as the composition of the produced gases, calculated by CASMO. Thus, it can be concluded that release took not place preferentially from the pellet periphery,

Table 5
Results of fission gas analysis.

Rod		WZtR165	WZR0058
Assumed burnup (MWd/kgU)		70.0	68.5
Assumed energy per fission (MeV)		200	200
Fission gas release (%)	Kr	7.56	7.77
	Xe	6.82	7.41
	Kr + Xe	6.88	7.43
Assumed energy per fission (MeV)		205.5	205.3
Fission gas release (%)	Kr	7.77	7.98
	Xe	7.00	7.61
	Kr + Xe	7.07	7.63
Isotopic composition of Kr (%)	^{80}Kr	0.002	0.004
	^{82}Kr	0.275	0.261
	^{83}Kr	8.392	8.554
	^{84}Kr	34.497	34.286
	^{85}Kr	5.540	5.396
	^{86}Kr	51.294	51.449
Isotopic composition of Xe (%)	^{128}Xe	0.073	0.069
	^{129}Xe	0.002	0.003
	^{130}Xe	0.239	0.223
	^{131}Xe	5.059	5.146
	^{132}Xe	24.032	23.991
	^{134}Xe	28.341	28.483
	^{136}Xe	42.253	42.085
Released volume (0 °C, 0.1 MPa) (cm^3)	Kr	25.2	25.9
	Xe	227.1	240.7

Table 6
Fission gas ratios.

	^{134}Xe/^{86}Kr	(^{83}Kr + ^{84}Kr)/^{86}Kr	(^{131}Xe + ^{132}Xe)/^{134}Xe
Measured			
WZtR165	4.98	0.84	1.03
WZR0058	5.14	0.83	1.02
Calculated (CASMO)			
WZtR165	5.64	0.84	1.03
WZR0058	5.60	0.83	1.03
In thermal fission of			
^{235}U	3.96	0.78	0.93
^{239}Pu	10.02	1.01	1.21

where the portion of Pu fissions is significantly larger, compared to the average.

5.2. Gamma scanning

Figs. 1–3 show axial ^{134}Cs and ^{137}Cs activity profiles measured by gamma scanning on rods WZtR165, WZR0058 and WZtR160. The shapes of the profiles are typical for PWR rods. Some caesium migration to the colder pellet interfaces has occurred, in particular in the upper part of the rods. Two gaps of about 0.5 mm were found in the fuel column of rod WZtR165 at an elevation of about 3570 mm. A similar gap had formed in rod WZR0058 as well at an elevation of 2390 mm. Such gaps are quite often observed. They form early in life during initial fuel densification, when a pellet gets stuck against the cladding wall, whereas the fuel stack below this position is still shrinking. Later on, all pellets get into hard contact with the cladding due to cladding creep-down and fuel swelling, which prevents these gaps from being closed again.

5.3. Isotope analysis

The isotopic composition of uranium and plutonium in all samples is compiled in Tables 7 and 8. The indicated uncertainty corresponds to the standard deviation calculated from five (uranium)
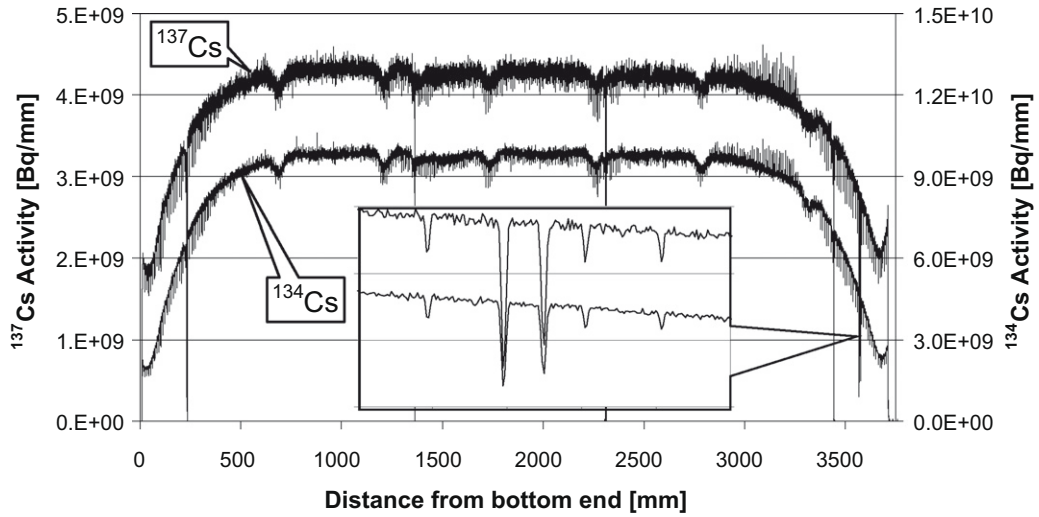
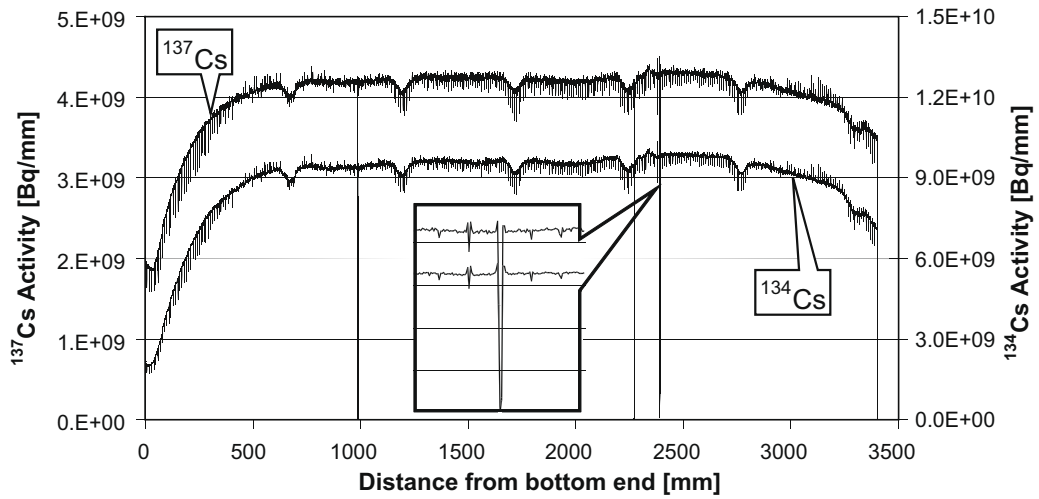**Fig. 1.** Axial profile of ^{134}Cs and ^{137}Cs in fuel rod WZtR165.

Fig. 2. Axial profile of ^{134}Cs and ^{137}Cs in fuel rod WZR0058.
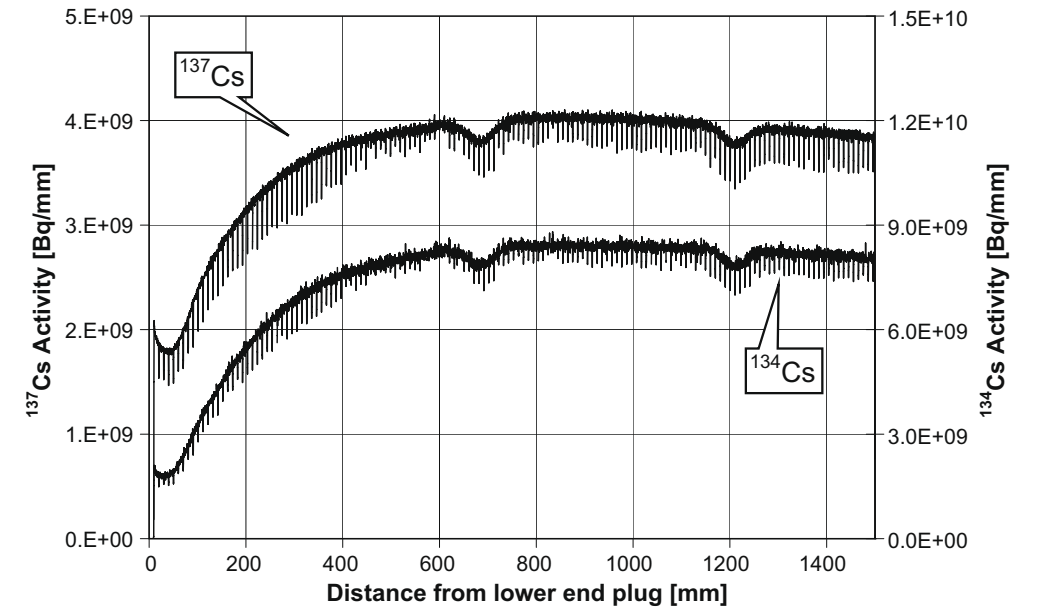

Fig. 3. Axial profile of ^{134}Cs and ^{137}Cs in lower part of fuel rod WZtR160.

Table 7
Isotopic composition of uranium.

Sample	Abundance (%)			
	^{234}U	^{235}U	^{236}U	^{238}U
E58-88 1st campaign	0.024	1.319	0.562	98.095
Uncertainty	0.002	0.064	0.023	0.080
E58-88 2nd campaign	0.027	1.374	0.671	97.928
Uncertainty	0.001	0.005	0.004	0.007
E58-148	0.023	0.918	0.681	98.378
Uncertainty	0.002	0.019	0.016	0.031
E58-257	0.022	0.571	0.768	98.639
Uncertainty	0.001	0.003	0.005	0.008
E58-263	0.016	0.525	0.675	98.784
Uncertainty	0.003	0.016	0.018	0.034
E58-773	0.014	0.321	0.644	99.016
Uncertainty	0.002	0.011	0.014	0.015
E58-793 1st campaign	0.015	0.313	0.683	98.988
Uncertainty	0.003	0.020	0.023	0.039
E58-793 2nd campaign	0.0193	0.343	0.773	98.864
Uncertainty	0.0001	0.003	0.005	0.003
E58-796	0.015	0.321	0.670	98.994
Uncertainty	0.002	0.011	0.014	0.013
WZtR165-2a	0.014	0.295	0.680	99.011
Uncertainty	0.002	0.010	0.014	0.019
WZtR160-800	0.020	0.397	0.786	98.796
Uncertainty	0.001	0.002	0.004	0.003

Table 8
Isotopic composition of plutonium.

Sample	Abundance (%)				
	^{238}Pu	^{239}Pu	^{240}Pu	^{241}Pu	^{242}Pu
E58-88 1st campaign	2.51	57.96	22.15	12.33	5.04
Uncertainty	0.06	0.27	0.08	0.08	0.06
at EOB	2.47	56.84	21.70	14.04	4.95
E58-88 2nd campaign	2.54	58.99	22.65	10.57	5.25
Uncertainty	0.09	0.44	0.20	0.24	0.13
at EOB	2.45	56.83	21.78	13.89	5.06
E58-148	3.30	52.46	23.82	12.99	7.43
Uncertainty	0.19	0.28	0.01	0.10	0.06
at EOB	3.23	51.42	23.29	14.79	7.28
E58-257 1st analysis	5.52	48.53	24.74	11.22	10.00
Uncertainty	0.10	0.11	0.20	0.06	0.15
at EOB	5.31	46.72	23.61	14.74	9.63
E58-257 2nd analysis	5.01	48.13	25.03	11.61	10.23
Uncertainty	0.22	0.86	0.16	0.46	0.47
at EOB	4.80	46.17	23.80	15.41	9.81
E58-263	4.86	47.53	24.18	13.39	10.05
Uncertainty	0.10	0.11	0.13	0.08	0.09
at EOB	4.76	46.59	23.56	15.24	9.85
E58-773	5.86	44.58	24.41	13.01	12.14
Uncertainty	0.19	0.15	0.09	0.11	0.16
at EOB	5.75	43.75	23.76	14.83	11.91
E58-793 1st campaign	6.03	44.51	24.19	13.16	12.11
Uncertainty	0.16	1.13	0.35	0.40	0.32
at EOB	5.92	43.66	23.56	14.99	11.88
E58-793 2nd campaign	5.90	44.99	25.10	11.35	12.66
Uncertainty	0.02	0.34	0.13	0.09	0.17
at EOB	5.68	43.37	23.82	14.92	12.20
E58-796	5.62	44.23	24.98	13.26	11.91
Uncertainty	0.26	0.49	0.16	0.28	0.15
at EOB	5.51	43.38	24.32	15.11	11.68
WZtR165-2a	5.85	44.45	24.15	13.15	12.41
Uncertainty	0.22	0.24	0.23	0.13	0.06
at EOB	5.74	43.62	23.48	14.99	12.18
WZtR160-800 1st analysis	5.98	44.75	26.14	11.07	12.06
Uncertainty	0.27	0.13	0.16	0.08	0.05
at EOB	5.76	43.15	24.88	14.57	11.63
WZtR160-800 2nd analysis	5.50	44.95	25.78	11.42	12.35
Uncertainty	0.03	0.07	0.01	0.05	0.02
at EOB	5.29	43.21	24.44	15.19	11.87

and three (plutonium) individual runs. The amount of ^{233}U was below the detection limit in all cases. The plutonium abundance values were corrected for the decay of ^{241}Pu and the amount of ^{240}Pu formed through decay of ^{244}Cm since the end of the irradiation and renormalized to 100%.

^{n}X/^{238}U values of all analysed isotopes are plotted in Figs. 4–16 as a function of burnup. Experimental data are represented by symbols that are depicted as a function of the burnup value based on gamma scanning. Values calculated by SAS2H for the end of the irradiation are represented by lines.

Uncertainties for individual data points were estimated according to the rules of error propagation, taking into account counting statistics as well as uncertainties of spike solution concentrations and isotopic compositions and of the spiking procedure. A summary of approximate estimated relative uncertainties is compiled in Table 9.
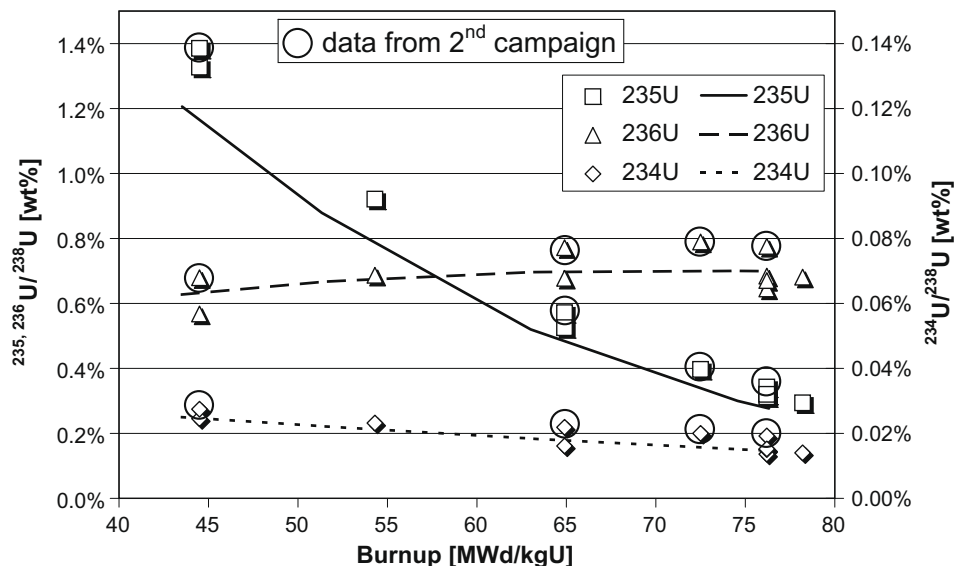

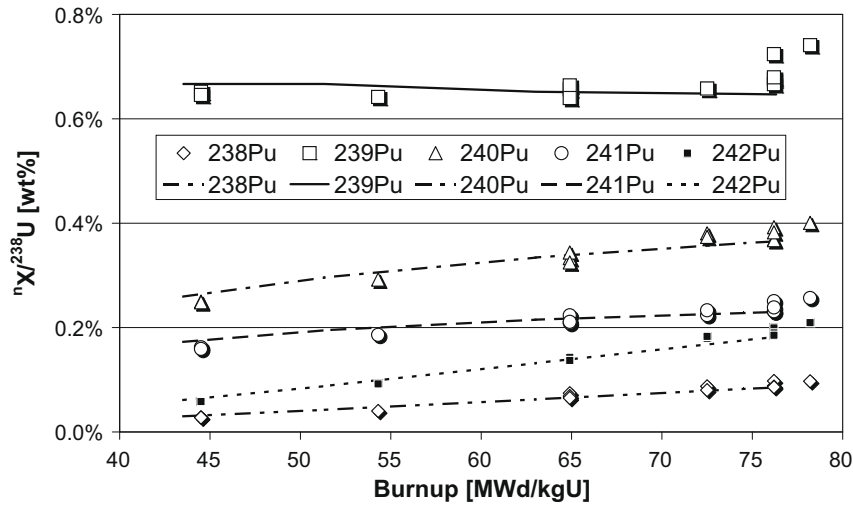**Fig. 4.** Content of uranium isotopes relative to ^{238}U.

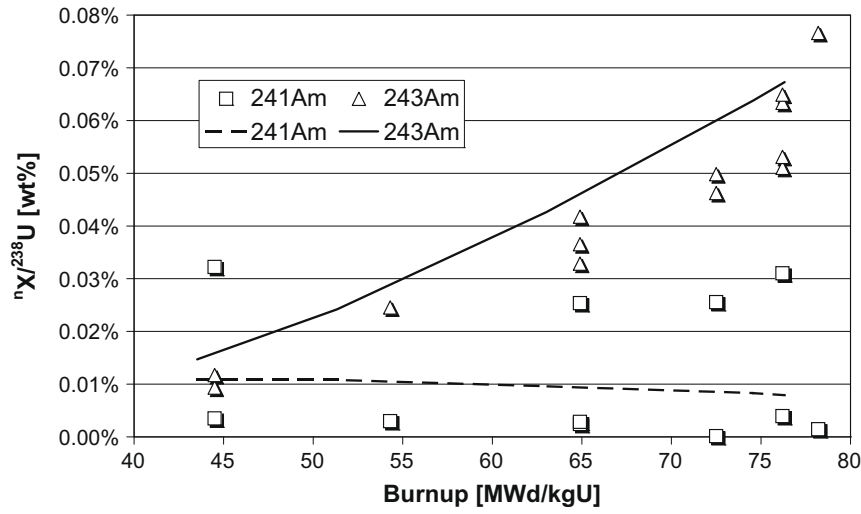**Fig. 5.** Content of plutonium isotopes relative to ^{238}U.

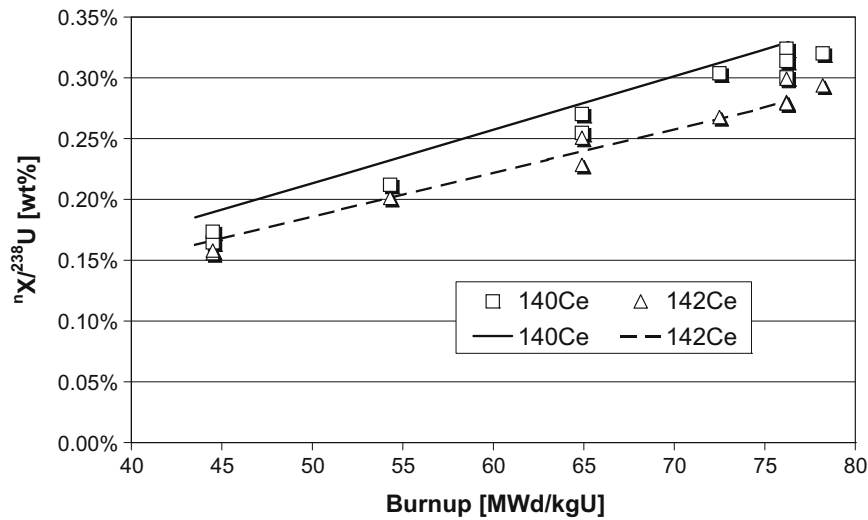**Fig. 6.** Content of ^{241}Am and ^{243}Am relative to ^{238}U.

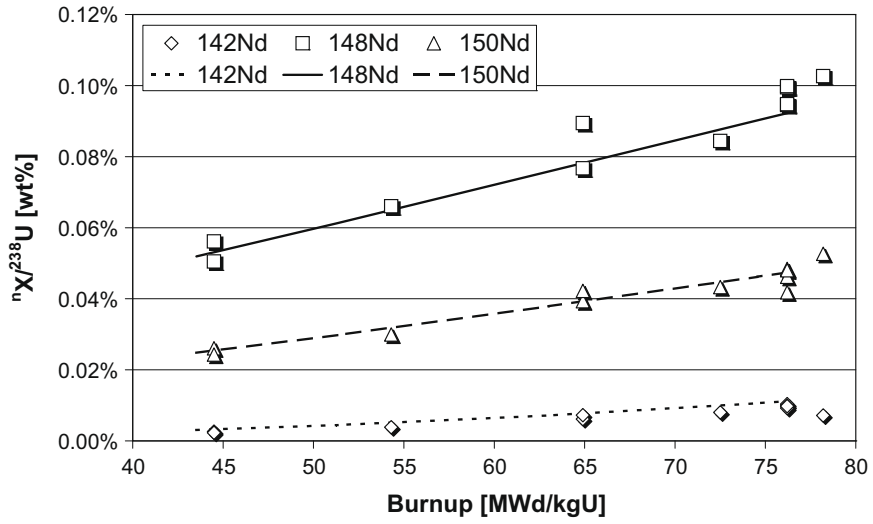**Fig. 7.** Content of ^{140}Ce and ^{142}Ce relative to ^{238}U.

Fig. 8. Content of ^{142}Nd, ^{148}Nd and ^{150}Nd relative to ^{238}U.
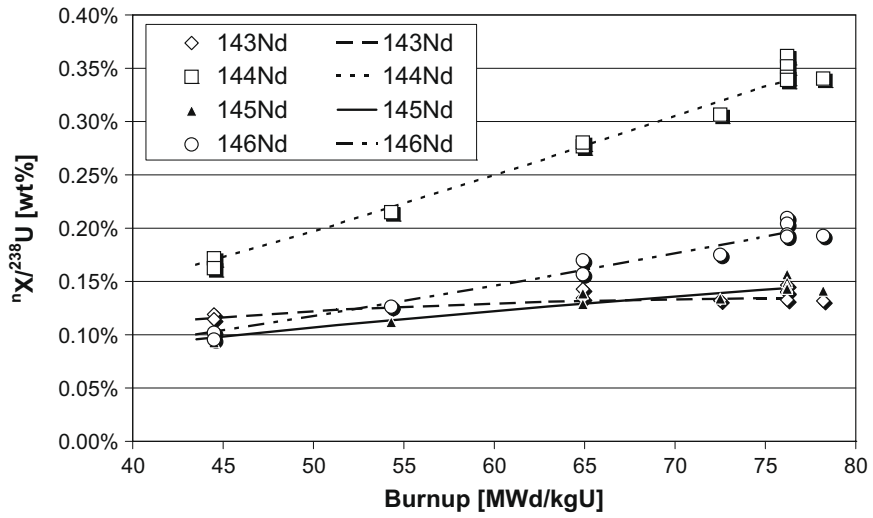
Fig. 9. Content of ^{143}Nd, ^{144}Nd, ^{145}Nd and ^{146}Nd relative to ^{238}U.
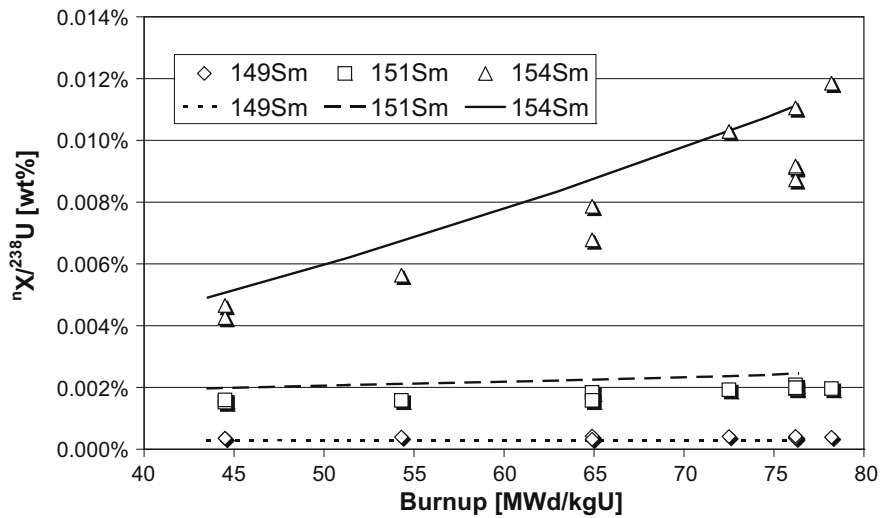
Fig. 10. Content of ^{149}Sm, ^{151}Sm and ^{154}Sm relative to ^{238}U.
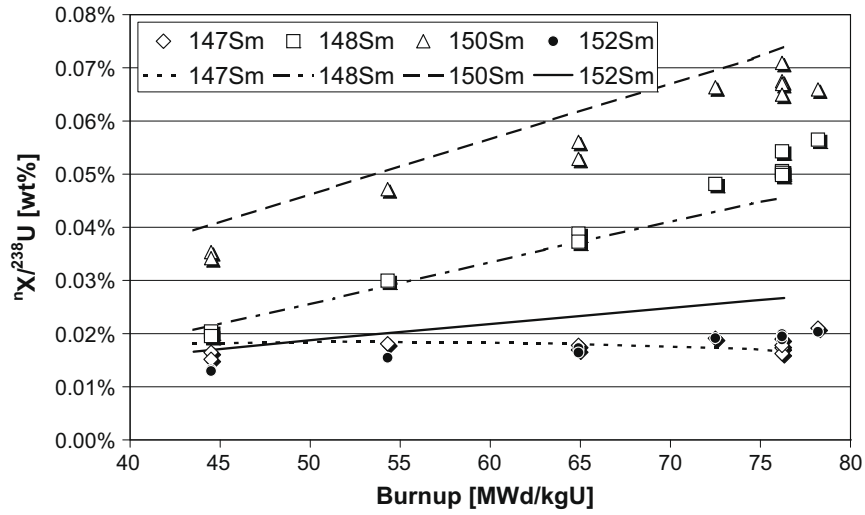
Fig. 11. Content of ^{147}Sm, ^{148}Sm, ^{150}Sm and ^{152}Sm relative to ^{238}U.
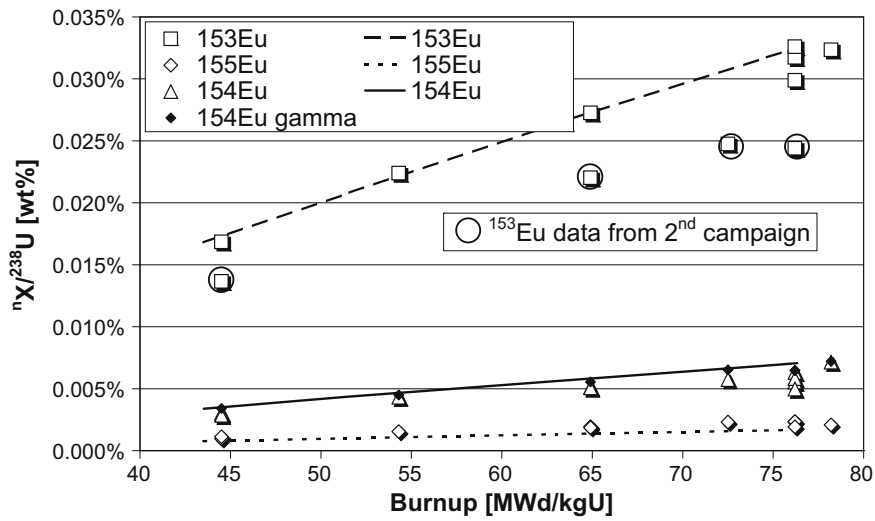
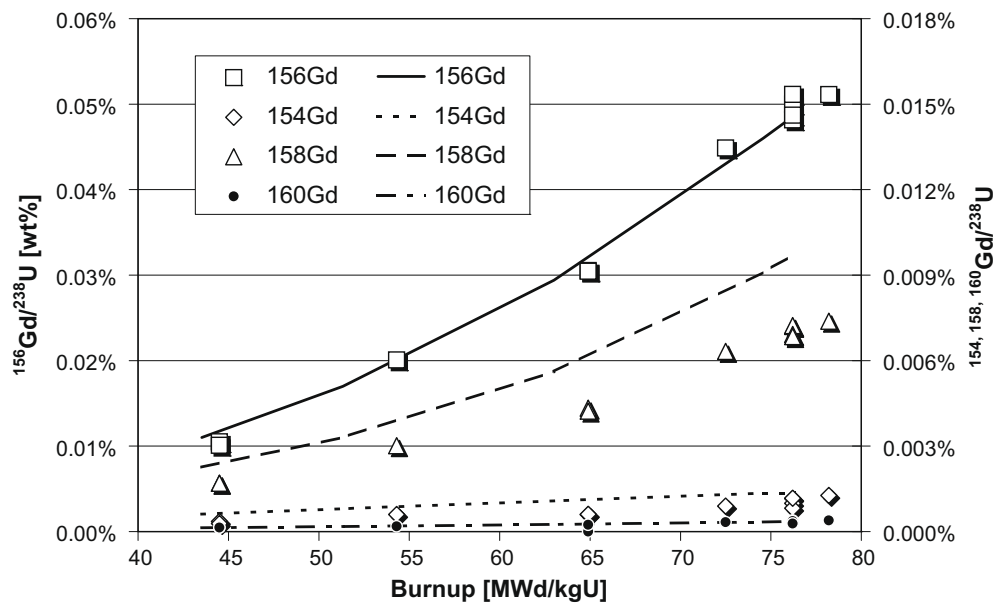**Fig. 12.** Content of europium isotopes relative to ^{238}U.

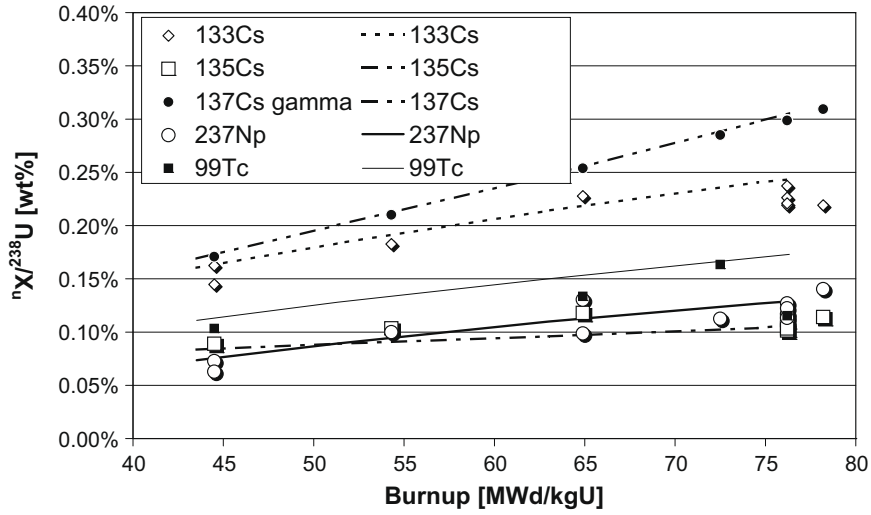**Fig. 13.** Content of gadolinium isotopes relative to ^{238}U.

Fig. 14. Content of ^{99}Tc, ^{133}Cs, ^{135}Cs, ^{139}La and ^{237}Np relative to ^{238}U determined by one-point calibration analysis and of ^{137}Cs based on gamma scanning data.
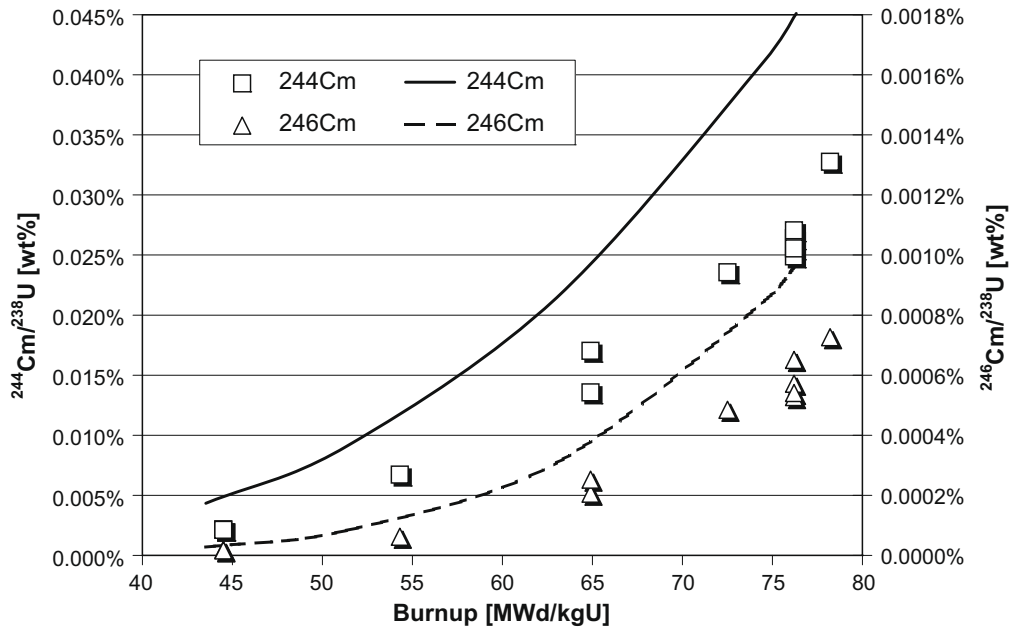

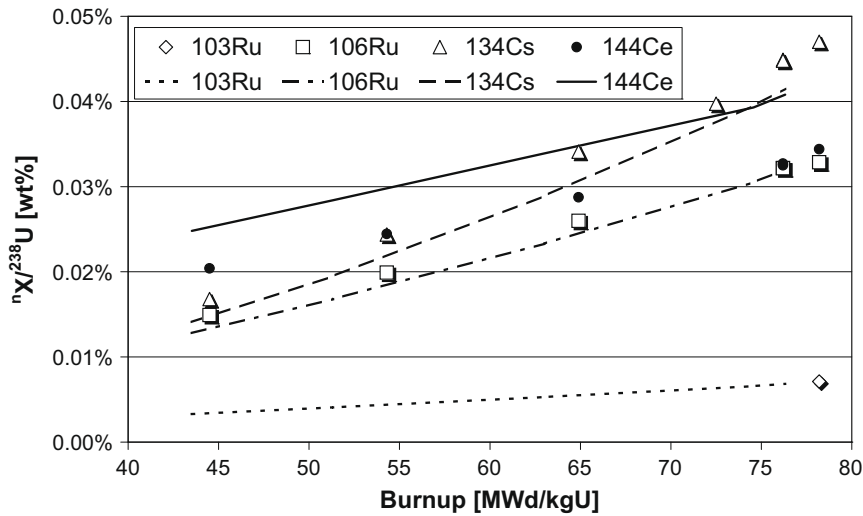**Fig. 15.** Content of ^{244}Cm and ^{246}Cm relative to ^{238}U determined by one-point calibration analysis.

Fig. 16. Content of ^{103}Ru, ^{106}Ru, ^{134}Cs and ^{144}Ce relative to ^{238}U, based on gamma scanning data.

Provided that the fuel solutions from the first campaign that were reanalysed had been stable, performance of the two equipments can be compared. By comparing the two data sets from samples E58-257 and E58-263, even performance of different dissolution methods and the potential impact of different sample size can be assessed. Only in two cases, there seems to be a difference between data from the first and the second campaign. ^{234}U, ^{235}U and, most pronounced, ^{236}U values from the second campaign are systematically higher, compared to data from the first campaign (Fig. 4). This might have been caused by an improper intercalibration of the two different modes applied for assessing ^{238}U on one hand and the minor uranium isotopes on the other hand.

The second case concerns ^{153}Eu (Fig. 12). Results from the second campaign seem to be systematically lower than those from the first campaign, whereas all other europium data form a consistent set of data. The reason is not known.

Table 9
Approximate uncertainties (1σ) of ^{n}X/^{238}U values for all analysed isotopes.

Isotope	Uncertainty, relative (%)	Method
^{234}U	13	IDA/ICP-MS
^{235}U	5	
^{236}U	5	
^{238}U	2	
^{238}Pu	7	IDA/HPLC–ICP-MS
^{239}Pu	4	
^{240}Pu	4	
^{241}Pu	4	
^{242}Pu	4	
^{237}Np	8	One-point calibration
^{241}Am	5	IDA/HPLC–ICP-MS
^{243}Am	5	
^{244}Cm	10	One-point calibration
^{246}Cm	15	
^{99}Tc	8	One-point calibration
^{103}Ru	10	Gamma scan
^{106}Ru	10	
^{133}Cs	8	One-point calibration
^{134}Cs	10	Gamma scan
^{135}Cs	8	One-point calibration
^{137}Cs	5	Gamma scan
^{139}La	8	One-point calibration
^{140}Ce	4	IDA/HPLC–ICP-MS
^{142}Ce	4	
^{144}Ce	10	Gamma scan
^{142}Nd	5	IDA/HPLC–ICP-MS
^{143}Nd	4	
^{144}Nd	4	
^{145}Nd	4	
^{146}Nd	4	
^{148}Nd	5	
^{150}Nd	5	
^{147}Sm	5	IDA/HPLC–ICP-MS
^{148}Sm	5	
^{149}Sm	10	
^{150}Sm	5	
^{151}Sm	6	
^{152}Sm	5	
^{154}Sm	5	
^{153}Eu	6	IDA/HPLC–ICP-MS
^{154}Eu	6	
	15	Gamma scan
^{155}Eu	8	IDA/HPLC–ICP-MS
^{154}Gd	6	IDA/HPLC–ICP-MS
^{156}Gd	5	
^{158}Gd	5	
^{160}Gd	6	

The plutonium data are summarised in Fig. 5. The amount of ^{241}Pu was decay-corrected back to the end of irradiation. The small portion of ^{240}Pu formed through decay of ^{244}Cm between the end of irradiation and the date of analysis was calculated on the basis of the experimentally determined amount of ^{244}Cm and subtracted from the analysed ^{240}Pu value. The apparent sharp increase of the ^{239}Pu content at high burnup is most probably not a burnup effect, but a consequence of the fact that the samples stem from three different rods. They had reached almost the same burnup, but under slightly different conditions and with slightly deviating irradiation histories. This leads to different nuclide inventories, in particular when production is sensitive to differences in the neutron spectrum. Overall, plutonium data form a consistent set and are in good agreement with calculated values.

Fig. 6 shows americium data. Experimental and SAS2H ^{243}Am values give a consistent picture and trends and discrepancies observed for these isotopes are also consistent with the experimental spent fuel benchmark bibliography [12–14]. Even here, the apparent sharp increase at high burnup is a consequence of small differences in operating conditions of the three mother rods. In contrast to ^{243}Am, ^{241}Am does not exhibit a consistent pattern. The amount that was formed through decay of ^{241}Pu between the end of irradiation and the date of the analyses represents a significant portion of the analysed amount of ^{241}Am. Thus, even a small relative error in the plutonium analysis leads to a large uncertainty in the amount of ^{241}Am present at the end of irradiation. Methods with significantly higher accuracy and precision would be necessary for analysing ^{241}Am in fuel samples with a decay time of several years.

The analysis of cerium has often caused problems due to unidentified reasons, sometimes leading to bad reproducibility and a large scatter in both, the isotopic ratio and the analysed amount. Nevertheless, the set of data presented in Fig. 7 is quite consistent and in good agreement with SAS2H data. ^{144}Ce data are shown in Fig. 16. The analysed amount of ^{144}Ce at the end of irradiation follows the same burnup trend as the SAS2H calculations, but with about 25% lower values than calculated.

^{144}Nd is subject to a decay correction. The amount formed through decay of ^{144}Ce between the end of irradiation and the date of analysis was calculated based on the analysed amount of ^{144}Ce and subtracted from the analysed ^{144}Nd amount. The neodymium data shown in Figs. 8 and 9 form a consistent set and are in good agreement with the code calculation predictions.

Samarium data are shown in Figs. 10 and 11. A significant amount of the analysed ^{147}Sm, about 40% in the first campaign and 50% in the second campaign, was formed through decay of ^{147}Pm between the end of irradiation and the analysis date. The corresponding correction of the experimental values was based on the amount of ^{147}Pm calculated by CASMO. When comparing samarium data to SAS2H results, it should be kept in mind that most isotopes have large thermal neutron capture cross sections or that they are formed through chains with nuclides with large cross sections. Overall, the samarium data at the end of irradiation are in agreement with the experimental values and the trends and differences observed are consistent with the experimental spent fuel benchmark bibliography [12–14].

^{154}Eu was analysed with two independent methods, gamma scanning and IDA. As illustrated in Fig. 12 the values are very similar for the two measurement methods and are in good agreement with SA2H calculations.

SAS2H results for gadolinium isotopes show good agreement with experimental values, although ^{158}Gd is overestimated, as illustrated in Fig. 13.

Comparison of the analysed ^{99}Tc amounts with SAS2H predictions (Fig. 14) shows agreement in two cases and a large difference in one case. At low burnup (sample E58-88), alloy particles are still

Table 10
Experimental burnup values based on gamma scan and on comparison of analysis results with CASMO, compared to values derived from core design data and plant operating records.

Sample	Gamma scan value	Burnup (MWd/kgU) based on			Weighted average Nd values	Based on abundance of		Overall weighted average	Core design and plant data
		$^{146}Nd/^{238}U$	$^{148}Nd/^{238}U$	$^{150}Nd/^{238}U$		^{235}U	^{239}Pu		
E58-88 1st c.	44.5	44.7	46.2	45.8	45.4	42.4	43.0	43.7	43.5
Uncertainty	2.2	0.9	1.1	1.6	0.7	1.3	0.4	0.5	–
E58-88 2nd c.	44.5	42.1	41.6	43.0	42.2	41.3	43.0	41.9	–
Uncertainty	2.2	0.7	0.9	0.8	0.5	0.2	0.7	0.3	–
E58-148	54.3	53.7	54.1	51.7	53.2	51.8	53.2	52.7	51.3
Uncertainty	2.3	1.0	1.4	1.3	0.7	0.5	0.5	0.3	–
E58-257	64.9	64.1	62.4	65.4	63.9	62.8	64.6	63.7	–
Uncertainty	2.8	0.8	1.4	1.6	0.7	0.3	0.3	0.3	–
E58-263	64.9	68.3	72.4	69.2	69.8	64.5	64.8	65.8	63.0
Uncertainty	2.8	1.1	1.4	1.3	0.7	0.6	0.3	0.3	–
E58-773	76.2	80.4	79.9	74.7	78.3	74.5	73.8	74.9	74.5[a]
Uncertainty	3.3	1.8	2.4	2.0	1.2	0.6	0.5	0.5	–
E58-793 1st c.	76.2	78.8	80.1	77.7	78.9	74.9	74.1	76.2	74.5[a]
Uncertainty	3.3	2.6	3.5	3.3	1.8	1.4	3.9	1.5	–
E58-793 2nd c.	76.2	75.9	76.1	77.3	76.3	73.3	75.5	74.4	–
Uncertainty	3.3	0.8	1.3	1.8	0.8	0.3	1.3	0.5	–
E58-796	76.2	75.3	76.3	68.7	73.3	74.5	75.1	74.2	74.5[a]
Uncertainty	3.3	1.4	1.8	1.5	0.9	0.6	1.9	0.7	–
WZtR165-2a	78.2	75.5	82.3	83.3	79.4	76.2	74.3	76.3	76.3
Uncertainty	3.4	1.4	3.2	2.1	1.4	0.7	0.8	0.6	–
WZtR160-800	72.5	70.0	68.5	70.6	69.8	70.3	76.1	72.9	–
Uncertainty	3.1	0.8	1.9	2.1	1.0	0.3	0.3	0.3	–

[a] The burnup from these samples was very similar, thus average value was used.

small enough to be dissolved completely, which is not the case in sample E58-793 (burnup 76.2 MWd/kgU). In sample E58-257 (burnup 64.9 MWd/kgU), alloy particles were not completely dissolved either, but the undissolved portion was probably rather small. Sample WZtR160-800 was dissolved with an alternative method, where alloy particles were completely dissolved.

Experimental curium data show the same burnup trend as the code prediction curves, but are over predicted by ≈40% on average (Fig. 15), which is not consistent with the generally observed trends in the bibliography [12–14]. However, in view of the number of nuclear reactions involved in curium formation, agreement between experimental and modelling data may be acceptable.

The experimental data for the nuclides analysed by gamma scanning (Figs. 16 and 14 for ^{137}Cs) give a consistent picture, and deviations from predicted values are not very large.

The molybdenum analysis, performed in two samples only, was impacted by a significant contamination of natural molybdenum with unknown origin. The attempt to correct the data properly was not successful.

5.4. Burnup

All burnup data are compiled in Table 10. Weight factors proportional to the reciprocal absolute error were used for calculating the different weighted average values. Due to the low error compared to other individual values, the weighted average is somewhat dominated by ^{235}U. The indicated uncertainties do not include any uncertainty of CASMO calculations.

Even if individual values are different in the strict sense, considering the indicated (1σ) uncertainties, the overall picture is rather consistent. The fact that ^{235}U analysed in the second campaign might be systematically high, as discussed above, means that the corresponding burnup values might be slightly underestimated. Comparison of results from samples supposed to have the same burnup reveals that the bias is not more than about 3%.

The burnup data based on gamma scan and on comparison of experimental results with CASMO presented in Table 10 are very consistent and in good agreement with the burnup values derived independently, as described in Section 4.5, from core design data and plant operating records presented in the last column of this table.

6. Conclusions

The activities reported in this work are part of a high burnup fuel demonstration programme carried out at the Spanish Vandellós 2 pressurised light water reactor during cycles 7–11. Various methods applied to perform and analyse different sample measurements have been presented.

- Puncturing of irradiated fuel rods, gas sampling and mass spectrometric analysis of the gas composition is a well established standard technique for determining the portion of fission gases released to the free rod volume.
- Axial gamma scanning is routinely applied as well for determining the profile of some fission products and for establishing the basis for defining the exact cutting positions for samples to be destructively characterised. In addition, Studsvik quantitatively evaluates gamma scanning data, in order to determine local burnup and isotopic content of gamma emitting nuclides.
- In chemical analysis of dissolved fuel samples, gravitational chromatography for separating single elements followed by Thermal Ionisation Mass Spectrometry is a well established, very accurate and precise but time-consuming method. Studsvik applies an alternative method, High Performance Liquid Chromatography (HPLC) for elemental separations, combined with Inductively Coupled Plasma Mass Spectrometry (ICP-MS). This method is somewhat less precise. This disadvantage is at least partly compensated by the possibility of analysing a larger number of nuclides and samples.

In total, the content of more than 50 isotopes of 16 different elements was determined successfully in nine different fuel samples. In general, these over 400 data points give a consistent picture of

the isotopic content of irradiated fuel as a function of burnup. Only in a few cases, the analysis provided unexpected results that seem to be wrong, in most cases due to unidentified reasons.

Consistency checks of the measured isotope abundances and sample burnup have been performed with different depletion codes to assess both, the input data used to analyse experimental results and the experimental results themselves.

Sample burnup analysis was performed by comparing experimental isotopic abundances of uranium and plutonium composition as well as neodymium isotopic concentrations with corresponding CASMO based data. The results were consistent with values derived independently from gamma scanning and from core design data and plant operating records.

Measured isotope abundances have been assessed using the industry standard SAS2H sequence of the SCALE code system. The aim of this analysis was twofold: (1) to serve as an independent validation check for the results obtained with new equipment and (2) to identify potential limitations and/or biases of this widely used tool to accurately predict isotopic inventories for high burnup fuel. This exercise showed good agreement between measured and calculated values for most of the analysed isotopes, similar to those reported previously for lower burnup ranges. Thus, it could be concluded, that:

- SAS2H results for high burnup samples up to 70 MWd/kgU and in most cases even up to 76 MWd/KgU are not subject to higher uncertainty and/or different biases than for lower burnup samples,
- the different isotopic experimental measurement methods provide accurate results with acceptable precision.

Disclosure statement

This project has been designed, coordinated and managed by J.M. Conde, C. Alejano, M. Quecedo, M. Lloret and J.A. Gago, each representing their respective organizations. The experimental work of the project, as well as the data reduction and interpretation, has been performed by H.U. Zwicky, J. Low and M. Granfors. Calculations using the SAS2H sequence have been performed by C. Casado and J. Sabater. The manuscript has been drafted by H.U. Zwicky, and has been reviewed, corrected and accepted by all the authors.

All the authors have been working at their respective organizations for more than 3 years. The relationships of any nature with other people or organizations established during this period have not inappropriately influenced the work performed in this project.

The objective of this project is to measure basic nuclear data that could be used for the validation and assessment of fuel depletion codes. The organizations funding the project are a Government Agency and two Public Companies, and have no vested interest in the specific data values obtained, further than assuring that their quality is the highest possible. Due to the public origin of the project funding, the results are published in the open arena for general knowledge, analysis and final use.

Based on these statements, it is concluded that it does not exist any real or potential conflict of interest related to any of the authors.

References

[1] I.C. Gauld, J.C. Ryman, Nuclide Importance to Criticality Safety, Decay Heating, and Source Terms Related to Transport and Interim Storage of High-Burnup LWR Fuel, NUREG/CR-6700, Oak Ridge National Laboratory, January 2001.
[2] S. Röllin, et al., Determination of lanthanides in uranium materials using high performance liquid chromatographic separation and ICP-MS detection, in: G. Holland (Ed.), Recent Advances in Plasma Source Mass Spectrometry, 1994, pp. 28–35.
[3] J. Magill, G. Pfennig, J. Galy, Karlsruher Nuklidkarte (Chart of the Nuclides), seventh ed., 2006.
[4] Standard Test Method for Atom Percent Fission in Uranium and Plutonium Fuel (Neodymium-148 method), ASTM Standard E-321-96.
[5] Standard Test Method for Atom Percent Fission in Uranium and Plutonium Fuel (Mass Spectrometric Method), ASTM Standard E 244-80, 1995 (Withdrawn 2001).
[6] H.U. Zwicky, J. Low, A. Lidén, G. Lysell, D. Schrire, Burnup determination in irradiated fuel by means of isotopic analysis compared to CASMO calculations, Water Reactor Fuel Performance Meeting, Kyoto, Japan, October 2–6, 2005.
[7] SCALE: A Modular Code System for Performing Standardized Computer Analyses for Licensing Evaluation, NUREG/CR-0200 (ORNL/NUREG/CSD-2) Rev. 6 September 1998.
[8] H.U. Zwicky, J. Low, Fuel Pellet Isotopic Analyses of Vandellós 2 Rods WZTR165 and WZR0058, Final Report, Studsvik Technical Report N(H)-03/069 Rev. 1, April 2008.
[9] H.U. Zwicky, J. Low, Fuel Pellet Isotopic Analyses of Vandellós 2 Rods WZTR165 and WZR0058, Complementary Report, Studsvik Technical Report N(H)-04/135 Rev. 1, April 2008.
[10] R. Manzel C.T. Walker, High burnup fuel microstrucure and its effect on fuel rod performance, in: ANS International Topical Meeting on Light Water Reactor Fuel Performance, Park City, Utah, April 10–13, 2000.
[11] T.R. England, B.F. Rider, Evaluation and Compilation of Fission Product Yields 1993, LA-UR-94-3106, ENDF-349, Los Alamos National Laboratory, October 1994.
[12] ORNL/TM-12667, Validation of SCALE System for PWR Spent Fuel Isotopic Composition Analyses, March 1995.
[13] ORNL/TM-13317, An Extension of the Validation of SCALE (SAS2H) Isotopic Predictions for PWR Spent Fuel, September 1996.
[14] NUREG/CR-6798 (ORNL/TM-2001/259), Isotopic Analysis of high-Burnup PWR Spent Fuel Samples from the Takahama-3 reactor, January 2003.